

# Facility development update: The Kerr-gated Raman/ ultrafast time-resolved fluorescence instrument

Contact [igor.sazanovich@stfc.ac.uk](mailto:igor.sazanovich@stfc.ac.uk)

I. V. Sazanovich, G. M. Greetham, B. C. Coles, I. P. Clark, P. Matousek, A. W. Parker, and M. Towrie

Central Laser Facility, Research Complex at Harwell, Rutherford Appleton Laboratory, Harwell, OX11 0QX, U. K.

## Introduction

Optical Kerr gating relies on a transient birefringence induced in the Kerr material induced by an intense laser beam, placed between two crossed polarisers. This enables the external signal beam to pass through the crossed polarisers for the duration of the gating laser pulse acting on the Kerr medium. The first application of an optically driven Kerr-gate to remove fluorescent backgrounds from (resonance) Raman spectra was conceptually proposed in 1980's by Deffontaine et al.<sup>1</sup> The concept was experimentally developed in 1999 at the CLF by utilizing the benefits of regenerative amplifier technology operating at 1 kHz repetition rate and demonstrated ~40% gate opening efficiency<sup>2-4</sup>. Over the years, this facility yielded numerous high-profile publications.<sup>5</sup> The Kerr gate has continued to be developed and the ULTRA laser system<sup>6</sup> has recently enabled us to upgrade the facility to 10 kHz improving signal-to-noise and/or data acquisition times. In this report we present the description and current specifications of the upgraded setup along with examples of the data taken.

## Instrument design

The Kerr-gating setup is driven by the picosecond arm of the ULTRA laser system<sup>6</sup> which delivers ~ 6 W at 10 kHz at ~ 800 nm, with the pulse width ~ 1 ps. About 350 mW of fundamental is split with a beam sampler to generate ~120 mW of 2<sup>nd</sup> harmonic (400 nm) in a Type I BBO crystal and used as a Raman probe.

The general layout of the Kerr gate is shown on Figure 1. The Kerr gate comprises two crossed polarisers P1 & P2 with a Kerr cell in-between (quartz cell filled with carbon disulfide, 2 mm path length). The entrance and exit polarisers P1 & P2 are set to transmit horizontal and vertical polarization, respectively, as the spectrograph was found to have higher transmission for vertically polarized light (by about 15%). In the current setup we use polarisers of 25 mm aperture (Halbo Optics PS25). The extinction ratio of the open/closed Kerr gate is ~ 10<sup>5</sup>.

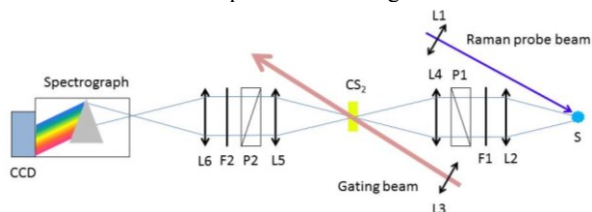


Figure 1. Schematic diagram of the Kerr-gate, where: S – sample, L1 – L6 – lenses, F1, F2 – cut-off filters, P1, P2 – polarisers, CS<sub>2</sub> – the Kerr cell filled with carbon disulfide. See text for further details.

To activate the Kerr gate, we use ~ 4 W (0.4 mJ) of fundamental beam (800 nm), brought down with the lens L3 (250 mm focal length) to a spot of approximately 2 mm diameter on the Kerr cell (the focal point itself is placed approx. 20 mm behind the Kerr cell). It was found that tighter focusing of gating beam though providing higher gate opening efficiency causes spectral shift and broadening of Raman lines at time delays immediately following the time zero. The polarization of the gating beam is set at 45° to that of the polarisers P1 & P2.

The Raman scattering and/or fluorescence of the sample S is initiated with the 400 nm beam, focused with the lens F1 (300 mm focal length) to a spot size of ~ 100 μm diameter on the sample. In the Kerr-gated Raman experiments, the arrival time of the Raman signal to the Kerr cell has to be precisely matched with the picosecond gating pulse which is coordinated by sending the 400 nm beam via an optical delay line comprising a hollow retroreflector and a motorized linear stage (IMS-600LM from Newport, 600 mm travel range). The set-up can also be used for Time-Resolved Fluorescence (TRF) experiments, with a 4 ps response time, as the timing control between the 400 nm and the gating beams enables following the temporal evolution of fluorescence from the sample. For Kerr-gated Raman experiments, the polarization of the 400 nm beam is set to be parallel with the transmission axis of the entrance polariser; while for TRF experiments it is set at 54.7° (“magic angle”) to avoid contributions from rotational diffusion of the sample effecting the TRF dynamics.

Raman and fluorescence signals from the sample are collected and collimated with the lens L2 (F/1.7, 50 mm focal length), then passed through the long pass filter F1 (407 nm RazorEdge filter, LP02-407RU, Semrock) to block the Rayleigh scattering. The tilt angle of F1 is slightly adjusted to match the actual wavelength of the 400 nm beam. The collimated signal light comes onto the entrance polariser P1 and the lens L4 (125 mm focal length) which images the signal light into the Kerr cell. After passing through the Kerr cell, the signal is re-collimated with the lens L5, identical to L4, and sent on to the exit polariser P2. The size of polarisers (25 mm) limits the aperture of the signal beam propagating through the optics.

When the Kerr gate is open it acts as a transient half waveplate rotating the polarization of the signal light, which is then transmitted by the exit polariser P2. After that, the collimated signal beam passes through the short-pass filter F2 (which is a combination of two Notch-Plus filters for 400 nm & 800 nm, both from Kaiser Optical Systems) to block mainly the scattered 800 nm light of the gating beam, and is then focused onto the entrance slit of the spectrograph with the lens L6 (100 mm focal length). Initially we attempted to use short-pass filters from Semrock (either 680 nm or 770 nm BrightLine short-pass). However the residual “oscillatory” transmission profile of those filters induced significant distortions to the spectral response, albeit providing higher extinction of 800 nm scattered light. The signal light passed through the Kerr gate is dispersed and detected with an F/4, ~ 300 mm focal length Czerny-Turner spectrograph (Shamrock 303i, Andor) equipped with a CCD camera (iDus DU-420A-BU2, Andor). The spectrograph has a triple-grating turret; the gratings routinely used in Kerr-gated Raman and TRF experiments are 1200 l/mm (500 nm blazed) & 150 l/mm (500 nm blazed), respectively. The CCD has a 1024 x 256 pixels (26 μm pixel size) silicon sensor, 16 bit ADC, and is Peltier-cooled. The CCD is operated in the vertical binning mode, and has software selectable region of interest optimised on signals to minimise dark noise and cosmic rays. The experiment control software is written in LabVIEW and provides full control of the hardware settings & data acquisition, with the exception of the spectrograph control, which is performed from Andor software.

## Performance specifications

For 400 nm Raman excitation the 1200 l/mm grating provides  $\sim 67 \text{ nm}/3500 \text{ cm}^{-1}$  coverage in Raman mode, and the 150 l/mm grating provides 600 nm coverage in TRF mode. The spectral resolution of the setup in Raman mode is  $\geq 15 \text{ cm}^{-1}$  and is limited by both the laser bandwidth ( $\sim 15 \text{ cm}^{-1}$ ) and the resolution of the spectrograph ( $\sim 12 \text{ cm}^{-1}$ ). The low frequency limit in Raman mode is  $\sim 500 \text{ cm}^{-1}$  with the currently used long-pass filter. The sensitivity of the setup is sufficient to operate even at the narrowest slit size ( $20 \mu\text{m}$ ), being able to saturate the detector with the Kerr-gated Raman signal of a solvent in 20-30 s at 0.5  $\mu\text{J}$  excitation pulse energy. Signal intensity significantly increases when expanding the slit size to  $60 \mu\text{m}$ , at this setting the broadening of the Kerr-gated Raman lines due to the slit size becomes noticeable. The routinely achievable dark noise level in Kerr gated experiments is  $\sim 6$  counts rms in 10 s acquisition. The typical pulse energy of the 400 nm beam delivered to the sample is 0.1 to 0.5  $\mu\text{J}$  and in this geometry is limited by photostability and non-linear effects in the sample. The gate opening efficiency is  $\sim 40\%$  as estimated by measuring gated/non-gated (when both polarisers P1&P2 set parallel to each other) Raman signal of neat solvents and correcting for grating response. The temporal response of the setup for optically dense samples is estimated  $\geq 4$  ps (as illustrated by Figure 2). For the transparent samples, the temporal response is several picoseconds longer due to the sample thickness effect (samples are up to 0.5 mm thick).

## Kerr-gated Raman of RuOEP(C=O) in acetonitrile

In Figure 2 we present the Kerr-gated resonance Raman data for Ru(II) octaethyl porphyrin carbonyl (RuOEP(C=O) for short) in acetonitrile, at 1.8 mM concentration.

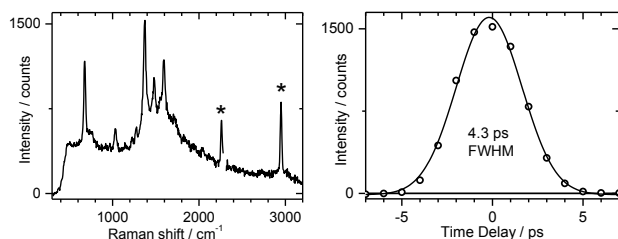


Figure 2. Kerr-gated resonance Raman data for RuOEP(C=O) in acetonitrile. Left panel: the spectrum at zero time delay (when the signal reaches maximum). The asterisks denote solvent Raman lines. Right panel: temporal profile of the signal plotted for  $1371 \text{ cm}^{-1}$  Raman band (circles) obtained through delaying Raman probe pulse vs. gating pulse. The solid line represents Gaussian fit.

The Kerr-gated Raman spectrum shows well-resolved resonance Raman lines of the porphyrin along with the most intense Raman features of the solvent. The Raman line positions agree well with literature data<sup>7</sup>. A high optical density ( $\text{OD} \sim 5$  at 400 nm in 0.3 mm) gave short optical pathlength in the sample enabling the technical limit of the temporal response of the instrument to be reached.

## Time-Resolved Fluorescence of Fluorescein in EtOH

Figure 3 demonstrates the power of the Kerr gate in acquiring a Raman spectrum from a strongly emissive fluorescent dye Fluorescein in ethanol with and without the gate. The emission yield of fluorescein approaches 0.8 and without the gate emission completely obscures the Raman signatures (blue line) but with the gate (red line) the Raman lines of the solvent are easily observed.

Kerr-gating intrinsically offers also a capability of taking broadband time-resolved emission spectra with ultrafast temporal resolution. In Figure 4, we illustrate this additional capability by taking the TRF data for Fluorescein in ethanol. At early time delays TRF spectra show a fast spectral evolution in the 400 – 480 nm range, and also sharp Raman lines from the solvent.

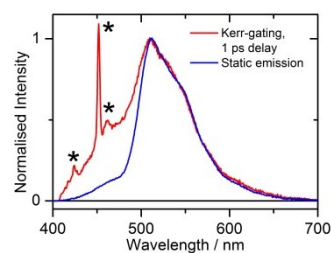


Figure 3. Comparison of the Kerr-gated spectrum taken at 1 ps time delay (red line) from Fluorescein in ethanol with the reconstructed steady-state spectrum from the same sample (blue line). Both spectra have been normalized to the peak intensity of fluorescence.

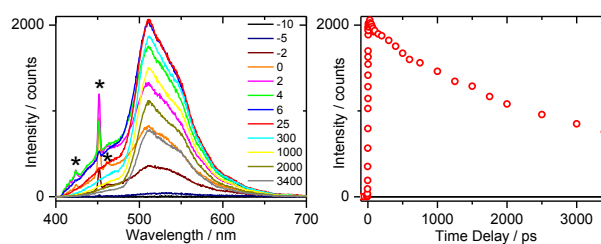


Figure 4. TRF data for Fluorescein in ethanol. Left panel: the set of TRF spectra at representative time delays. The asterisks denote Raman lines from the solvent. Right panel: The temporal evolution of the fluorescence plotted at the maximum of spectrum.

The Raman signal disappears within several picoseconds in accord with the temporal response of the setup, and it is only fluorescence signal observed at later time delays up to  $\sim 3.5$  ns limit of the optical delay line. The corresponding fluorescence decay curve is plotted on the right-hand panel which shows gradual decay in accord with the fluorescence lifetime of  $\sim 4$  ns.

## Conclusions

The Kerr-gating facility has been developed for 10 kHz repetition rate and implemented in ULTRA facility. The upgraded setup demonstrates 40% gate opening efficiency,  $\sim 4$  ps gate width, and can cover a spectral window  $\sim 3000 \text{ cm}^{-1}$  in one frame with  $\sim 15 \text{ cm}^{-1}$  spectral resolution in the Raman experiments. The instrument provides efficient rejection of the emission background in Raman experiments, and offers a capability to carry out broad-band TRF experiments with ultrafast temporal resolution. Development is on-going to enable the tunable excitation and bring Time-Resolved resonance Raman capability to the facility.

## References

1. A. Deffontaine, M. Delhaye and M. Bridoux, In *Time-resolved Vibrational Spectroscopy*. A. Laubereau and M. Stockburger, Eds. (1985), Springer: Berlin, 20–24.
2. P. Matousek, M. Towrie, A. Stanley and A.W. Parker, *Applied Spectroscopy*, **53**, 1485, (1999).
3. P. Matousek, M. Towrie, C. Ma, W. M. Kwok, D. Phillips, W. T. Toner and A. W. Parker, *J. Raman Spectroscopy*, **32**, 983, (2001).
4. P. Matousek, M. Towrie and A. W. Parker, *J. Raman Spectroscopy*, **33**, 238, (2002).
5. S. K. Sahoo, S. Umopathy and A. W. Parker, *Applied Spectroscopy*, **65**, 1087, (2011).
6. G. M. Greetham, P. Burgos, Q. A. Cao, I. P. Clark, P. S. Codd, R. C. Farrow, M. W. George, M. Kogimtzis, P. Matousek, A. W. Parker, M. R. Pollard, D. A. Robinson, Z. J. Xin and M. Towrie, *Applied Spectroscopy*, **64**, 1311, (2010).
7. G. A. Schick and D. F. Bocian, *J. Am. Chem. Soc.*, **106**, 1682, (1984).